Progress Report

Transport and Nucleation Processes in the Vapor Growth of Diamond

DARPA University Research Initiation Grant

No: N00014–89J–3167

John C. Angus, Principal Investigator
J. Adin Mann, Jr., Co–Principal Investigator
Yaxin Wang
Mahendra Sunkara
Paul A. Washlock
Maria Kuczmarski
Zhidan Li

January 31, 1991

REPORT DOCUMENTATION PAGE

Form Approved
OMB No. 0704-0188

1. AGENCY USE ONLY (Leave blank)	2. REPORT DATE	3. REPORT TYPE AND DATES COVERED
	January 31, 1991	Progress, 7/1/89-12/31/90

4. TITLE AND SUBTITLE
Transport and Nucleation Processes in the Vapor Growth of Diamond

5. FUNDING NUMBERS
N00014-89J-3167
PE 06011030
R & T du 89002-02
Work Unit 02

6. AUTHOR(S)
John C. Angus, J. Adin Mann Jr., Yaxin Wang, Mahendra Sunkara, Paul A. Washlock, Macia Kuczmarski, Zhidan Li

7. PERFORMING ORGANIZATION NAME(S) AND ADDRESS(ES)
Case Western Reserve University
2040 Adelbert Road
Cleveland, OH 44106

8. PERFORMING ORGANIZATION REPORT NUMBER

9. SPONSORING/MONITORING AGENCY NAME(S) AND ADDRESS(ES)
DARPA/Office of Naval Research
800 North Quincy St.
Arlington, VA 22217

10. SPONSORING/MONITORING AGENCY REPORT NUMBER

11. SUPPLEMENTARY NOTES
Defense Advanced Research Projects Agency University Research Initiative Grant

12a. DISTRIBUTION/AVAILABILITY STATEMENT
Approved for public release: Distribution Unlimited

12b. DISTRIBUTION CODE

13. ABSTRACT (Maximum 200 words)

Rule-based computer modelling has been used to study the initial stages of diamond nucleation from the vapor and the relationship of observed crystalline morphology to the nucleation and growth mechanisms. The enhanced growth rates of nuclei with multiple twins has been confirmed and plausible mechanisms for the formation of five- and twenty-fold twinned crystals found. Two-dimensional simulations of a hot-filament reactor are being made. The flow field, temperature field and species concentrations for reactors of arbitrary geometry are obtained. At present the chemical reaction mechanism is restricted to ten simultaneous reactions. The program is being further modified to handle more complex chemistry. Experimental work on the seeding of diamond nucleation with specific compounds has proceeded in parallel with the modelling studies. This work was done in cooperation with Dr. Michael Geis of the MIT Lincoln Laboratories. The compound 3, 4, 9, 10-perylene tetracarboxylic acid dianhydride was found to be a strong nucleation promoter, while adamantane and its derivatives were not.

14. SUBJECT TERMS	15. NUMBER OF PAGES
Diamond, chemical vapor deposition, nucleation, reactor modelling	34
	16. PRICE CODE

17. SECURITY CLASSIFICATION OF REPORT	18. SECURITY CLASSIFICATION OF THIS PAGE	19. SECURITY CLASSIFICATION OF ABSTRACT	20. LIMITATION OF ABSTRACT
Unclassified	Unclassified	Unclassified	UL

ABSTRACT

This is an interim progress report on DARPA University Research Initiation Grant, "Transport and Nucleation Processes in the Vapor Growth of Diamond." Significant progress has been made in three areas: 1) computer modelling of diamond nucleation and growth, 2) computer modeling of the hot–filament reactor, 3) seeding experiments.

Rule–based computer modelling of diamond growth has been used to study the initial stages of diamond nucleation from the vapor and the relationship of observed crystalline morphology to the nucleation and growth mechanisms. The enhanced growth rates of nuclei with multiple twins has been confirmed and plausible mechanisms for the formation of five– and twenty–fold twinned crystals found. Work has been initiated to cast the crystal growth modelling into the theoretical formalisms provided by molecular dynamics methods.

We are working with a supplier of a commercial fluid mechanics program to provide modifications which will permit use of the program to model diamond deposition reactors. This work is being performed in collaboration with the NASA Lewis Research Center. We are currently using the model to provide two–dimensional simulations of a hot–filament reactor. The flow field, temperature field and species concentrations for reactors of arbitrary geometry are obtained. At present the chemical reaction mechanism is restricted to ten simultaneous reactions. The program is being further modified to handle more complex chemistry.

Experimental work on the seeding of diamond nucleation with specific compounds has proceeded in parallel with the above two modelling studies. This work was done in cooperation with Dr. Michael Geis of the MIT Lincoln Laboratories. The compound 3, 4, 9, 10–perylene tetracarboxylic acid dianhydride was found to be a strong nucleation promoter, while adamantane and its derivatives were not. A special hot–filament reactor with movable shutter, rotating substrate holder, and continuously variable substrate–filament distance was designed and constructed for this work. The results have potential importance for both practical applications in which enhanced nucleation density is desired and also in providing insight into the nature of the chemical processes that lead to diamond nucleation.

Digital Equipment Corporation has provided high level work stations with advanced graphics capability in support of our efforts on the modelling of diamond nucleation and growth processes.

The work described in this progress report was directed by Professors John C. Angus and J. Adin Mann, Jr. Dr. Yaxin Wang, Mr. Paul Washlock, Mr. Mahendra Sunkara, Ms. Maria Kuczmarski and Ms. Zhidan Li all contributed to parts of the research.

TABLE OF CONTENTS

1.0 INTRODUCTION

This is an interim report describing progress made under the DARPA University Research Initiation Grant "Transport and Nucleation Processes in the Vapor Growth of Diamond." The purposes of this research are to obtain a comprehensive, integrated understanding of the complex dynamic processes which take place during chemical vapor deposition of diamond. The processes studied under the grant include: 1) transport of heat and chemical species, 2) kinetics of complex hydrocarbon reactions, 3) dynamics of surface transport, 4) dynamics of diamond nucleation and growth and 5) the relationship of these factors to the nature of the diamond deposit. Other purposes of the grant include the education of graduate students and the enhancement of the capabilities for advanced modelling and simulation of chemical vapor deposition processes at Case Western Reserve University.

Very significant progress has been made on all aspects of the research. A summary of the results obtained to date is given in the following sections of the report.

2.0 MODELLING OF DIAMOND NUCLEATION AND GROWTH

2.1 General Description of Computer Program

One major effort has been the development of a computer program for the modelling of atom addition during diamond growth. In particular, we compare the observed morphologies of diamond crystals grown in the laboratory to the morphologies of crystals "grown" on the computer with known stacking errors. Correlation of experimentally observed morphologies with morphologies obtained with known atom addition rules on the computer can give important clues about nucleation and growth mechanisms.

The algorithm is both very simple and very powerful. In the present version all carbon atoms are assumed to have tetrahedral, sp^3, coordination. An ad–atom bonded once to the surface has limited rotational freedom about the bond axis, i.e., its orientation can be either staggered or eclipsed. These two orientations correspond respectively to chair or boat six–membered rings. The eclipsed orientation (boat conformation) is a stacking error in the diamond–cubic lattice. The relative probabilities of the staggered and eclipsed orientations can be fixed by the program user. Also, if desired, stacking errors at specific points in the precursor nucleus can be introduced.

The program makes provision for atom removal as well as atom addition. The relative overall probability of atom removal can be adjusted so that it is less than, equal to, or greater than the probability of atom addition. These three conditions correspond to growth, equilibrium and evaporation of the crystallites.

A basic assumption of the modelling is that the atom addition and removal events occur randomly on the crystal surface according to a Poisson process. Multiple atom events are not normally allowed. It is possible, however, to provide for simultaneous two–atom addition events. This is necessary, for example, to simulate acetylene addition at step sites.

The program is sufficiently general that it can be used to test the influence of different kinetic mechanisms on crystalline morphology. Different mechanisms, for example attachment of CH_3 radicals or C_2H_2 molecules, may have differing probabilities of attachment at different sites. Different probabilities can be entered into the program and the influence on crystallite morphology and growth rates determined.

It is necessary to account for several complex affects that can arise from the interaction of various stacking errors. For example, some atoms that are not fully bonded to four other carbon atoms, will be buried in the crystal as the simulation proceeds. These buried free bonds must be automatically removed from the table which contains the free surface bonds. Also, intersections of growth fronts arising from different stacking errors will sometimes lead to bond distances and bond angles that are "close" but not equal to the single carbon–carbon bond parameters. In this case, the program must determine whether or not a bond should be formed. The most common situation when this occurs is the formation of five–membered rings.

2.2 Flowsheet of Simulation Programs

A flow sheet of the simulation program is given in Figure 1. The program is written in Fortran 77 and is implemented on a Digital Equipment Vaxstation 3100.

A brief description of the various elements of the simulation is given below.

1) The precursor molecule (nucleus) is defined. The nucleus may be a molecule, e.g., bicyclodecane or adamantane, or any fragment of a diamond lattice with or without stacking or other errors. The spatial coordinates of each atom and the direction cosines of each free surface bond are stored in the computer as tables. Each free surface bond is a potential site for the addition of a carbon atom.

2) A surface atom is selected using a uniform random number generator. If used without modification, this procedure will choose pendant carbon atoms (bonded once to the surface and having three free bonds) three times more often than atoms on a smooth {111} surface, which are bonded three times to the surface with one free bond.

3) A uniform random number generator is used to decide whether or not the selected atom leaves the surface or not. The probabilities of atom removal decrease exponentially with the number of bonds made to the rest of the nucleus. (See Section 2.3 below.)

4) The uniform random number generator is used to chose another vacant surface site, i.e., a free bond.

5) An adatom is added to the selected surface site. The adatom is assumed to have hindered rotational freedom about its bond axis, i.e., it can select either the staggered or the eclipsed bond orientation. The relative probabilities of the two orientations are pre–selected by the operator of the program. The choice between the staggered and eclipsed conformations is made using the uniform random number generator.

6) The nearest neighbors to the ad–atom are examined. If any of the free bonds of a nearest neighbor are colinear with one of the free bonds of the ad–atom, then a bond is formed. These two free bonds are removed from the growth site table.

   (An alternate procedure available to the operator is to have the program test both possible orientations of the adatom. In this procedure the presence of an appropriately oriented nearest neighbor fixes the orientation of the ad–atom rather than the random number generator. In this variation the random number generator is used only to select the orientation of ad–atoms without nearest neighbors.)

7) In some situations no colinear nearest neighbor free bonds are present even though the bond distance requirement is met. In this case these free bonds are sterically hindered and are removed from the growth site table. In physical terms they would be buried in the crystal as free radical sites (or bonds terminated with hydrogen).

8) Atoms at the next–nearest neighbor positions from the ad–atom are also examined. In certain situations the distance and orientation of the next–nearest atom are "close" to that of the standard bond length and orientation. This occurs most commonly at the intersection of two stacking errors on {111} surfaces that are inclined by 70°53′. A bond can be formed at this intersection giving rise to a strained five–membered ring. The program permits specification of a range of bond lengths and bond angles over which a bond may be formed.

2.3 Atom Removal Algorithm

The atom removal algorithm is quite simple and is based on previous work by the principal investigator (4). The probability of removal, P_n, of an n–bonded atom is proportional to a first order rate constant k_n. These rate constants are assumed to depend only on the number of bonds the surface atom makes with the rest of the lattice. The probability of removal decreases as the number of bonds, n, to other carbon atoms is increased, i.e.,

$$P_4 < P_3 < P_2 < P_1 \qquad (1)$$

The probabilities of atom removed, P_n, are assumed to be related to the bond energy, E, through an Arrhenius expression.

$$k_n = A \exp\left[\frac{-nE}{RT}\right] \qquad (2)$$

where A is a constant. Initially, we assume that $P_4 = P_3 = 0$. In this approximation, the ratio of rate constants for removal of two bonded and singly bonded atoms is simply:

$$\frac{k_2}{k_1} = \exp\left[\frac{-E}{RT}\right] \qquad (3)$$

The relative probability of atom removal is fixed by equations (2) and (3) above.

2.4 Modelling Results

The program was tested using a single carbon atom (methane equivalent) as the nucleus and various ratios of probabilities of the staggered and eclipsed conformations of ad–atoms. The results are shown in Figure 2.

Figure 2a shows the resulting structure when there is 0% probability of forming an eclipsed bond. As expected, a perfect diamond–cubic crystal is grown. Figures 2b, 2c, 2d and 2e show the resulting structures when the probabilities of an eclipsed bond (stacking error) are 10%, 25%, 50% and 100% respectively. Figure 2b shows a crystallite with a single stacking error while Figures 2c, 2d and 2e become progressively more disordered. Figures 2d and 2e contain numerous five–membered rings and atoms with incomplete bonding. These

two cases are probably not physically significant and in those situations sp^2 (trigonal) coordination of the carbon atoms likely arises.

Figure 2f shows a small fragment of the network in 2e. It is an incomplete icosahedron made up entirely of five–membered rings.

Runs were made using nuclei with two parallel twin planes under various atom addition rules. In particular, the trans boat–boat conformer of bicyclodecane proposed by Angus et al. as a potential nucleus was used (1,2). This molecule is shown in Figure 3. The results of the simulation after growth to 200, 600 and 1000 atoms are shown in Figure 4. A plate–like structure evolves within the plane of the two stacking errors. This simulation was done using atom addition rules which favored two–atom addition events. Simulations done in which the atom–addition rules did not favor two–atom addition events led to octahedral shaped crystals containing a single micro–twin. These results are consistent with the earlier proposal (1,2).

Runs were also made with various nuclei having forced stacking errors along non–parallel {111} planes. Several of these nuclei are shown in Figure 5. This type of initial nucleus gives rise to complex multiply twinned crystals. The five–fold twinned decahedral crystal arising from the doubly twinned nucleus shown in Figure 5b is displayed in Figure 6. The five–membered rings closed at the center of the crystal according to the bond–length and bond–angle ranges initially specified. Closure was not achieved further from the center and the growth of a grain boundary between two of the five sectors of the crystal is evident.

2.5 Future Work

A major enhancement of the simulation will be the addition of an energy minimization program. After any atom is either added or removed, the atom positions will be placed in a molecular modelling program and the energy of the structure minimized. The up–dated atom coordinates will be returned to the crystal growing program. The energy minimization will be done using the program Chem–X from Chemical Design Incorporated. This program has been purchased under the DARPA URI grant and is running on a Digital Equipment Vaxstation 3100. It is highly likely that it will not be necessary to update the atom positions after every single event. It may only be necessary to do this after every 10 events for example. The energy minimization program will be of importance for generating realistic conditions for closure of five– and seven–membered rings and for rationalizing the structures of the smallest precursors.

Further enhancements of the program include the addition of a more detailed method of including hydrogen surface coverage and hydrogen abstraction reactions. With the present early version of the program, the influence of hydrogen surface coverage is subsumed within the probabilities assigned for atom addition.

Ultimately, we plan to add provision for sp^2 coordination of carbon atoms. This will probably, however, include only isolated sp^2 carbon sites (free radicals). Extended π–bonded structures will not be modelled.

3.0 MOLECULAR DYNAMICS ON DIAMOND SURFACES

3.1 Relationship to Nucleation and Growth Model

Sunkara and Angus have developed a rule–based algorithm for simulating diamond cluster growth under certain assumptions explained in section 2 of this report. We are

attempting to cast this model into well–defined theoretical formalisms developed for the study of dynamic molecular processes on surfaces. These efforts are described in this section and in section 3.2 below.

The technique used by Sunkara to code the crystal growth model involves two features: 1) neighborhood tables are used to track the vertex (carbon atoms) and edges (bonds) of the evolving three–dimensional graph that begins from the primitive precursor by 2) rule based addition of new vertices. Since edges (bonds) are of fixed length, it is useful to define two classes of edges: a free edge is not connected to a vertex (atom) whereas the tied edge connects two vertices and becomes a bond. The free edge may be thought of as a dangling bond. The rules have the structure: IF < neighbor condition of tied and free bonds around the carbon atom being added to the cluster > THEN < action of adding the atom with the free bonds having a specific orientation with respect to its neighborhood; a distribution function may be sampled > ELSE < an alternative orientation is entered in the neighborhood table.>

In this way various defects are introduced into the growing cluster. Indeed rules are required that allow bonds to deform slightly so as to obtain closure of most interior free bonds. Not all interior free bonds can be connected unless edges substantially longer than sp^3 bond lengths are used; such edges are left free. Molecular mechanics can be used to adjust the entire set of bond lengths and angles in the cluster so as to minimize the total energy. The resulting structure may represent a possible cluster from an ensemble. An extension of the set of rules now being programmed will allow both growth and etching conditions for a more realistic simulation.

The Sunkara program has provided insight into possible growth patterns including the effect of twin planes. However, the dynamics is not represented in the model. While certain of the rules incorporate random choices, the stochastic process is not yet well defined in the mathematical sense. Indeed, the rules should be formulated so that the cluster will evolve as a Markov chain leading to equilibrium states belonging to a well defined ensemble such as the canonical ensemble. We believe that this can be done.

3.2 Application of Theory of Interacting Particles

A second approach involves an extension of the theory developed by Ycart, Woyczynski, Szulga, Reazor and Mann (5) for studying adsorption to a lattice. Here we developed the mathematics of filling a lattice through the theory of interacting particles as developed recently in the mathematics literature. The postulates of the theory and the application to the diamond growth problem are described briefly below.

Let S be the set of all sites, i.e., vertices with edge count less than four. With each of them we associate 0 if it is empty, and 1 if it is occupied. Then the general configuration at time t, denoted by η_t, is an element of $\{0,1\}^S$. Note that this is a more formal way of expressing the Sunkara rules. While our original work (5) assumed a fixed lattice for convenience. The Sunkara rules generate a graph which is but a modest generalization of what are assumed in Ycart et al. (4 and references therein). The Sunkara configurations are represented by η_t.

We assume that η_t is a Markov process and evolves according to the following rules:

(1) The conditional probability of adsorption of a particle at a given site x, between times t and $t + \Delta t$, is

$$P[\eta_{t+\Delta t}(x) = 1 \mid \eta_t(x) = 0] = \lambda \Delta t + o(\Delta t), \tag{4}$$

where $\lambda \geq 0$ is the rate of birth at any site.

(2) The conditional probability of desorption of a particle at a given site x, between times t and $t + \Delta t$, is

$$P[\eta_{t+\Delta t}(x) = 0 \mid A_p(t,x)] = \mu_p \Delta t + o(\Delta t), \tag{5}$$

where the conditioning event $A_p(t,x)$ is "At time t, x is occupied and its neighborhood pattern is p," so that $\mu_p \geq 0$ is the rate of death of a particle in pattern p.

(3) If p and p′ are two neighborhood patterns such that p′ is obtained from p by adding a molecule on a free site, then $\mu_p \geq \mu_{p'}$.

Hypothesis (1) is equivalent to assuming that the interval of time between a desorption and the following adsorption at one given site has an exponential distribution with constant parameter. This is the case if we suppose that the particles, present in modest to small concentration in the fluid phase, strike the surface randomly, according to a Poisson process of rate Λ. The interval of time for the adsorption to occur at a given site is exponential with parameter $\lambda = \Lambda/N$.

Hypothesis (2) amounts to saying that the interval of time before a desorption at a given site is an exponential random variable with parameter μ_p, depending on the neighborhood pattern of the site. It can also be seen as the duration of life on the surface of a particle in pattern p and its expected value is $1/\mu_p$. Therefore, the monotonicity relation imposed by (3) accounts for the intuitive idea that the more a particle is surrounded by others, the more stable is its state, and thus the harder it is for the particle to desorb. This hypothesis makes our system what is usually called an attractive spin system, and it is an equivalent of an attractive adsorbate–adsorbate interaction. Not only does it correspond to a physical reality, but also it is most useful from a theoretical point of view.

Let us consider the case where all the rates μ_p are equal to μ. Then all the sites are independent. If n particles are present at a give time on the surface, then the interval of time before the next desorption is an exponential random variable with parameter $n\mu$. Hence, in this particular case, the number of particles present at one given time on the surface is the Markov process that has been studied by us in a previous publication. Its distribution at any instant of time and, virtually, every other variable associated with this model can be computed explicitly.

A number of the rules proposed by Sunkara and Angus describe what is called a conditioning event, Ap(t,x). Thus we have shown that the theory of Ycart et al. (5) provides the basis for a strict theory of diamond growth in the framework of the model described in section 3.1 of this report.

Our next step is the derivation of the rate equation for the hypothesis set out above. Formally this should go easily; the formulas we have previously derived must be modified taking into account the new configurations.

Then we will construct a program that will assemble diamond clusters according to these rules. But now the dynamics will have a physical correspondence with growth limited only by the assumptions of a Markov process. Once this program is operating we will be able to make explicit predictions of diamond growth that will be subject to experimental verification.

Clearly the parameters to be determined are λ, μ_p and the energy associated with each configuration that determines $A_p(t,x)$. Recent, unpublished work by a colleague (B.L. Granovsky) suggests that the "inverse" problem can be solved. That is given rate data the parameters λ, μ_p, ... can be determined and their uncertainties estimated. This hint will be investigated.

4.0 MODELLING OF HOT FILAMENT REACTOR

4.1 General Discussion of Reactor Modelling

Two methods are being used to model the processes taking place during diamond growth in a hot–filament reactor. The Chem–kin program developed by Sandia Laboratories has been obtained and is running on our computers. This program permits detailed study of the complex hydrocarbon chemistry taking place during diamond deposition. Multiple simultaneous reactions, including surface reactions, as well as diffusive and convective transport can all be handled by the set of Chem–kin programs. Chem–kin does not, however, permit detailed study of specific reactor geometries. For reactor modelling, therefore, we have selected a commercial program, FLUENT, developed by Creare Inc. of Hanover, New Hampshire.

FLUENT uses a finite difference method to solve the basic momentum conservation (Navier Stokes) equations for fluid flow. Three–dimensional and two–dimensional flows of essentially arbitrary geometry can be modelled. Additional conservation equations for energy and chemical species are used to treat energy transport and chemical reactions. Convective, conductive and radiative heat transfer and diffusive and convective transport of species are all treated by the program. Unfortunately, the FLUENT program as currently implemented can handle only rather simple chemistry. We are working with the NASA Lewis Research Center and Creare to upgrade the program so it is useful for simulations of the hot filament diamond deposition reactor.

The simulations shown in this report are all two–dimensional. Physically, this can be interpreted as flow through a channel with finite x (axial) and y (vertical) dimensions, but with an infinite width (normal to the x–y plane). The results given here, Figures 9 through 14, all show an x–y cross–section of this semi–infinite channel.

4.2 Simulations Without Chemical Reactions

Initially we performed two–dimensional simulations of our hot filament reactor with the chemistry turned off, i.e., the flow is comprised of pure H_2 only. The geometry of the hot–filament diamond deposition reactor being simulated is shown in Figure 7. A square grid with a cell side of 2 mm was used. Convergence of the solution is a major issue. Even without the chemical reactions, up to 9000 iterations are required to reach convergence.

The parameters used for the simulations are given in Table 1.

TABLE 1

Parameters used in Simulations*

Filament Temperature	2473° K
Substrate Temperature	1100° K
Wall Temperature	1000° K
Inlet Gas Temperature	1000° K
Pressure	20 Torr
Flow Rate	100 sccm
Inlet Velocity Profile	flat
Inlet Axial Velocity	$4.678 \times 10^{-2} \frac{m}{s}$
Channel Height	7.62 cm
Filament Perimeter	0.8 cm
Substrate Height	1.27 cm
Filament to Substrate Distance	0.8 cm
Inlet to Filament Distance	6.3 cm

* Unless specified on the Figure caption, the above parameters were used for all simulations.

One set of runs was done at a total pressure of 20 Torr and a second set at a total pressure of 760 Torr. These simulations were performed with the chemistry turned off, i.e., only pure H_2 was assumed to be present. The results of these simulations are shown in Figures 8 through 11. Comparison of the two sets of results shows the very strong influence of convection at 760 Torr compared to 20 Torr. It should be noted that the typical diamond growing conditions in a hot-filament reactor are between 20 and 100 Torr.

4.3 Simulations With Chemical Reactions

Detailed chemical mechanisms of the complex hydrocarbon chemistry involved at diamond synthesis conditions have been proposed by Harris (6) and Frenklach (7). The mechanism proposed by Harris includes 92 independent chemical reactions. The Frenklach mechanism has 158 gas phase and 52 surface reactions.

One of the main purposes of the present reactor simulation is to predict other ranges of operating parameters which can give rise to high concentrations of atomic hydrogen and

consequently, high growth rates. For these purposes it is probably not necessary to have a completely detailed kinetic mechanism which includes all trace species.

We are now introducing a set of reactions which includes the major processes taking place during diamond growth. These reactions are summarized below. On the hot filament one has the following reactions involving hydrogen:

$$H_2 \rightarrow 2H \qquad \text{(R1)}$$

$$2H \rightarrow H_2 \qquad \text{(R2)}$$

Also, on the hot filament one can have the fragmentation of hydrocarbons.

$$CH_4 \rightarrow CH_3 + H \qquad \text{(R3)}$$

$$C_2H_6 \rightarrow C_2H_5 + H \qquad \text{(R4)}$$

The principal homogeneous gas phase reactions involving only hydrogen are:

$$H + H + M \rightarrow H_2 + M \qquad \text{(R5)}$$

$$H_2 + M \rightarrow H + H + M \qquad \text{(R6)}$$

where M is any other molecule which can carry away or supply energy. The concentration of atomic hydrogen is strongly influenced by the presence of gaseous hydrocarbon species. For example, hydrogen atoms are destroyed by the following two gas phase reactions:

$$CH_4 + H \rightarrow CH_3 + H_2 \qquad \text{(R7)}$$

$$CH_3 + H + M \rightarrow CH_4 + M \qquad \text{(R8)}$$

Other gas phase reactions also are of importance. For example,

$$CH_3 + CH_3 + M \rightarrow C_2H_6 + M \qquad \text{(R9)}$$

and

$$CH_3 + CH_3 \rightarrow C_2H_5 + H \qquad \text{(R10)}$$

On the substrate surface one has both hydrogen addition and hydrogen abstraction, i.e.,

$$H + S \rightarrow HS \qquad \text{(R11)}$$

$$HS + H \rightarrow S + H_2 \qquad \text{(R12)}$$

Here S represents an active free site on the diamond surface. Other reactions involving hydrogen that will be subsequently added to the reaction set are:

$$HS \rightarrow H + S \qquad \text{(R13)}$$

$$S + H_2 \rightarrow HS + H \qquad \text{(R14)}$$

Two possible diamond forming reactions are initially being considered.

$$CH_3 + S \rightarrow CH_3S \qquad \text{(R15)}$$

and

$$CH_4 + S \rightarrow CH_3S + H \qquad \text{(R16)}$$

4.4 Changes in Reaction Mechanism

Since the current version of FLUENT is limited to only ten independent reactions, not all of the sixteen reactions listed above can be used at one time in the simulation. We are performing sensitivity tests to establish if any of the reactions in this set have negligible influence on the results. These reactions will be ignored in subsequent simulations. This procedure is not entirely satisfactory and one would like include many more reactions in the simulations. Despite the inability to use a comprehensive mechanism in the simulations, we believe that the ability to model real, arbitrary reactor geometries makes this approach a very useful complement to the comprehensive kinetic modelling possible in Chem–kin. Both approaches will have a role to play in the development of diamond chemical vapor deposition technology.

The concentration of atomic hydrogen at the heated filament is dominated by reactions R1 and R2. The rate constant for the dissociation of H_2 on a tungsten filament (reaction R1) was obtained from the literature (9). The rate constant for the reverse reaction (R2) was obtained using the equilibrium constant and the principle of detailed balance. The initial results from the simulations indicate that at the conditions normally encountered in hot–filament diamond deposition reactors the atomic hydrogen concentration at the filament is close to that predicted by equilibrium. Roughly speaking, this means that the rates of the chemical reactions (R1) and (R2) are sufficiently rapid to compensate for the depletion of atomic H by mass transport from the filament and by destruction through reactions such as (R5), (R7) and (R8). This will permit us to eliminate reactions (R1) and (R2) from the reaction, set and apply the equilibrium condition as a boundary condition at the filament.

The rate of the two diamond formation reactions (R15) and (R16) will be proportional to the fraction of the diamond surface that is not covered with hydrogen. The fractional hydrogen coverage is in turn fixed by reactions (R11), (R12), (R13) and (R14). If reactions (R11) and (R12) dominate, then a steady state fractional coverage is achieved in which the fractional hydrogen coverage is equal to $k_{11}/(k_{11} + k_{12})$. This approximation will permit us to eliminate several other reactions from the mechanism.

4.5 Testing of Reactor Simulations

The simulations were run for a variety of different reactor parameters. The rate constants for the homogeneous gas phase reactions were obtained from the Gas Phase Chemical Kinetics Data Base developed by the National Institute for Standards and Technology (8). The rate constants for the surface reactions were taken from the literature when available (9) or were estimated using kinetic theory collision rates and rate constants from comparable gas phase reactions.

All of the results shown in this report must be considered preliminary. We are still performing tests of the reaction mechanism and are checking values of the rate constants and diffusion coefficients.

Some of the preliminary results are shown in Figures 12 through 14. In Figure 12 the contours of constant mole fraction of atomic hydrogen are shown. Note that under these operating conditions, which are typical for a hot filament reactor, the mole fraction of H at

the filament closely approaches the value predicted by assuming equilibrium at the filament, i.e., $X_H = 0.143$ at 20 Torr and 2500° K.

Note that increasing the filament temperature from 2473 °K (Figure 12a) to 2800 °K (Figure 12b) increases the H atom fraction. The influence of increased pressure on the operation of the reactor is dramatic. This is shown in Figure 13 in which the temperature and H atom fraction contours are shown when the pressure in increased to 760 Torr (1 atm). The H atom fraction, shown in Figure 13b, is greatly reduced compared to the values shown in Figure 12a which were computed for the same filament temperature of 2473° K, but at a pressure of 20 Torr.

The influence of convective velocity and filament temperature is further explored in Figures 14a and 14b. In this simulation the filament temperature was reduced to 2000 °K and the convective velocity increased by a factor of 10 over the prior simulations.

The reactor modelling will also be tested in situations for which an analytical solution is available. We are currently investigating the reaction/diffusion problem from a heated wire with cylindrical symmetry and from a heated flat plate. The atomic hydrogen concentrations and temperatures predicted by the model will be compared to those from the analytical solution. This type of test can be used to check for programming and logic errors in the computer simulation, but cannot test for the validity of the chemical mechanism or the accuracy of the rate constants. (The same rate constants and simplified mechanism are used in both the simulation and the analytic solution.)

Finally, the results of the reactor simulation will be tested against real reactors. We will use values of hydrogen atom and methyl concentrations that have appeared in the literature (6,10,11,12).

4.6 Reactor Design Considerations

A major goal of the reactor modelling studies is to provide design criteria for guiding future reactor design. A number of useful observations have already been made which can be helpful in interpreting the results obtained from various types of diamond deposition reactors. These insights can be most easily be summarized through the use of three dimensionless groups which arise from a dimensional analysis of the basic conservation equations for the chemical species within the reactor.

The first dimensionless group is the Peclet number, Pe

$$Pe \equiv \frac{uL}{D} \tag{6}$$

where u is the convective velocity, L a characteristic length in the direction of species transport and D the diffusion coefficient. The Peclet number is a measure of the ratio of the magnitude of convective to diffusive transport.

The second dimensionless group is a Damköhler number, defined as

$$Dad \equiv \frac{kL^2}{D} \tag{7}$$

where k is a first order reaction rate constant. Dad is a measure of the rate of loss of a chemical species through chemical reaction to the rate of loss through diffusion. A second

Damköhler number measures the rate of loss by reaction to the rate of loss through convective transport.

$$Dac \equiv \frac{kL}{u} \tag{8}$$

From equations (6), (7) and (8) one immediately has

$$Dad = Pe\,Dac \tag{9}$$

Diamond deposition reactors operate under a very wide range of Pe, Dac and Dad. Angus et al. (13) have previously shown that typical hot–filament and microwave reactors operating, for example, at 20 Torr have $Pe << 1$, which indicates that the gas phase transport is dominated by diffusion. On the other hand, they showed that the atmospheric plasma jet reactors operate in a regime where $Pe >> 1$, indicating the gas phase transport is dominated by convection.

The values of Dad and Dac can be estimated for diamond deposition reactors. We focus attention only on the fate of atomic hydrogen after it is formed, for example at a hot filament. Reaction (R5) is assumed to be the dominant mechanism for the destruction of atomic hydrogen. A pseudo–first order rate expression is obtained by combining the rate expression for reaction (R5) with the equilibrium value for the atomic hydrogen concentration. We find that at temperatures on the order of 2000 °K and pressures of 20 Torr, that

$$Dad \cong 10^{-4}$$

$$Dac \cong 10^{-1}$$

$$Pe \cong 10^{-3}$$

For the above values we have assumed the characteristic length is equal to the filament to substrate distance, $L \cong 1$ cm, and a linear convective velocity of 1.0 cm/sec. The low value of Dad indicates that much of the atomic hydrogen formed by the hot filament will reach the vicinity of the substrate. If one increases the pressure to 760 Torr one has

$$Dad \cong 10^{-1}$$

which indicates significant destruction of atomic hydrogen in the region between the filament and substrate.

The above estimates include several serious approximations. They do, however, agree with the general trends observed in the simulations and in experimental reactors. See, for example, Figures 12a and 13b in which the atomic hydrogen mole fraction is compared at 20 Torr and 760 Torr.

Furthermore, we note that high convective velocities in atmospheric pressure reactors can lead to a reduction in Dac to the level where depletion of atomic hydrogen by reaction (R 5)is negligible compared to its rate of convective transport. In other words the convective velocity is sufficiently rapid to ensure transport of atomic H to the substrate before it is destroyed by reaction. It is indeed of interest that the reported atmospheric pressure processes all involve large convective velocities, which may be essential for their success. On the other hand, in the hot–filament and microwave reactors, the low pressure suppresses the rate of the termolecular destruction reaction (R 5) and provides a very high diffusion

coefficient. This combination of factors permits the atomic H formed at the filament to diffuse relatively long distances (L > 1 cm) before it is destroyed by reaction.

4.7 Future Reactor Modelling Studies

The simulations of specific reactor geometries can only be approximate because the computational burden is simply too great if both the exact geometry and the most complete set of chemical reactions are included. Nevertheless, we believe that a sufficiently accurate simulation will be achieved that will permit us to explore other operating regimes on the computer. We are interested in estimating the atomic hydrogen concentrations at significantly higher pressures than are commonly used and also estimating atomic hydrogen and methyl concentrations in unusual reactor geometries. A particular problem of interest is the influence of mixing when hydrogen and hydrocarbon streams are separately introduced into the reaction zone. Filament and reactor geometries that minimize loss of atomic hydrogen and hence increase energy efficiency can also be explored using the simulation. We believe the simulations will also be useful for the hot neutral gases leaving a thermal plasma region.

We also plan to move from two–dimensional modelling to full three–dimensional modelling. Realistic geometry, chemistry and three–dimensional simulation may require that the computations will be transferred to the Ohio Super Computer Center. In this situation, we will be using the work stations to set up and define the problem and as a smart interactive terminal. The computations themselves will be done on the supercomputer.

5.0 SEEDING EXPERIMENTS

5.1 Present Status

The work described in Section 5 of the report was done in collaboration with Dr. Michael W. Geis of the MIT Lincoln Laboratories.

Our studies have clearly shown that accurate estimations of nucleation density cannot be done without extremely precise control over the substrate–to–filament distance. Accordingly, a new reactor has been designed and constructed. This reactor has provision for a linear motion feed–through, which can be used to accurately position the substrate with respect to the filament. The substrate holder itself rotates during growth, which is required to achieve uniformity of conditions during the seeding experiments. Provision has also been made for a movable shutter, which reduces contamination from the filament.

A class of compounds has been proposed by the principal investigator as possible precursors to diamond nucleation. These are the multiply twinned, fully saturated polycyclic hydrocarbons. The simplest example is boat–boat bicyclodecane. It was proposed that these and related molecules are formed by hydrogenation of unsaturated or graphitic–like deposits in the atomic hydrogen environment (1,2). A certain fraction of the hydrogenated polycyclic compounds will have the necessary multiply twinned structure that is believed to be necessary for diamond nucleation. The compounds that are more closely related structurally to diamond, e.g., adamantane and its derivatives, would not be expected to be efficient nucleation promoters. This is because they have no easy site for atom addition. The multiply twinned precursors, on the other hand, have re–entrant surfaces which are continually renewed as growth proceeds. These re–entrant surfaces provide an efficient point for nucleation of new {111} layers.

To test this hypothesis, a series of seed molecules were added to a silicon surface. Silicon wafers were prepared by etching with HF followed by treatment with tetramethyl ammoniumhydroxide (TMAH) containing the seed molecule. Adamantane, adamantane carboxylic acid, adamantane amine and 3, 4, 9, 10–perylene tetracarboxylic acid dianhydride (PTCDA) were used as seed molecules. The adamantane and its derivatives did not promote nucleation; the PTCDA was a strong nucleation promoter. When PTCDA is used, the nucleation density (crystals per unit area) increases, and the average crystallite size decreases.

The structure of PTCDA is shown in Figure 15. One possible interpretation of the results is that the PTCDA was hydrogenated to a fully saturated structure, which in turn led to diamond nucleation. However, these results, while quite encouraging, are extremely preliminary. An alternative explanation for the results is that the adamantane and its derivatives, because of higher vapor pressures, were vaporized from the surface before they could serve as nucleation promoters.

5.2 Future Work

We plan to do carefully controlled experiments using a wide range of possible seed molecules of various structures and volatilities. Among the molecules to be tested will be the very long chain aliphatic acids, tetraphenyl and a series of compounds related to perylene. These experiments will be designed to test whether the nucleation rate is sensitive to particular molecular structures, or whether it depends solely on the availability of any carbon source on the substrate.

In addition there is the process of self–assembly in which various organic molecules can be chemisorbed on substrates to form structures with long range order. This technology has been developed for other purposes, but we believe it can be adapted to provide precursors of very well controlled structure and stability.

6.0 PUBLICATIONS

Several publications have arisen in full or in part from the work described in this report.

1. John C. Angus, Yaxin Wang and Mahendra Sunkara, "Metastable Growth of Diamond and Diamondlike Phases," accepted, Annual Reviews of Materials Science, 1991.

2. John C. Angus, Roy Gat, Zhidan Li, Mahendra Sunkara, Alfred B. Anderson, Satya Mehandru and Michael W. Geis, "Nucleation and Growth Processes in Chemical Vapor Deposition of Diamond," Electrochemical Society Second International Symposium on Diamond Materials, May 5–10, 1991, Washington, D.C.

3. Maria Kuczmarski, Paul Washlock and John C. Angus, "Modelling of Hot Filament Diamond Deposition Reactor," First International Conference on the Applications of Diamond Films and Related Materials," August 20–22, 1991, Auburn, Alabama.

7.0 FACILITIES

We have been extremely fortunate in receiving an External Research Program grant

from the Digital Equipment Corporation. This grant provided $307,000 worth of advanced workstations at a 75% discount. The workstations include advanced graphic capabilities. They provide us with state-of-the-art computation and graphics capabilities. The DARPA URI research support played an important role in our ability to secure this grant from the Digital Equipment Corporation.

8.0 REFERENCES

1. J.C. Angus, R.W. Hoffman and P. Schmidt, Proceedings of the First International Conference on the New Diamond Science and Technology, Tokyo, October, 1988.

2. M. Sunkara, J.C. Angus, C.C. Hayman, F.A. Buck, Carbon 28, 745 (1990).

3. S. Matsumoto and Y. Matsui, J. Mat. Sci 18, 1785–93.

4. J.C. Angus and T.J. Dyble, Surf. Sci. 50, 157 (1975).

5. B. Ycart, W.A. Woyczynski, J. Szulga, S. Reazor, and J.A. Mann "An Interacting Particle Model of Adsorption" Applicationes Mathematicae, 20 (3), 405 (1990).

6. S. J. Harris and A. M. Weiner, J. Appl. Phys. 67, 6520 (1990).

7. M. Frenklach and H. Wang, Phys. Rev. B 43, 1520 (1991).

8. NIST Chemical Kinetics Database, Version 2.0, National Institute of Standards and Technology, U.S. Department of Commerce.

9. M.U. Kislyuk and I.I. Tret'yakov, "Kinetics of the Heterogeneous Atomization of Hydrogen on Pure Metals," Translated from Kinetika i Kataliz, 18 (3), 577–579, May–June, 1977.

10. L. Schaeffer, U. Bringmann and C.P. Klages, Proceedings NATO Advanced Study Institute on Diamond and Diamondlike Materials, Castelvecchio Pascoli, Italy, 1990, to be published, Plenum Press.

11. F.G. Celii, P.E. Pehrson, H.T. Wang, J.E. Butler, Appl. Phys. Lett. 52, 2043 (1988).

12. S.J. Harris, A.M. Weiner, and T.A. Perry, Appl. Phys. Lett. 53, 1605 (1988).

13. J. C. Angus, F.A. Buck, M. Sunkara, T.F. Groth, C.C. Hayman and R. Gat, MRS Bulletin, 38 (October, 1989).

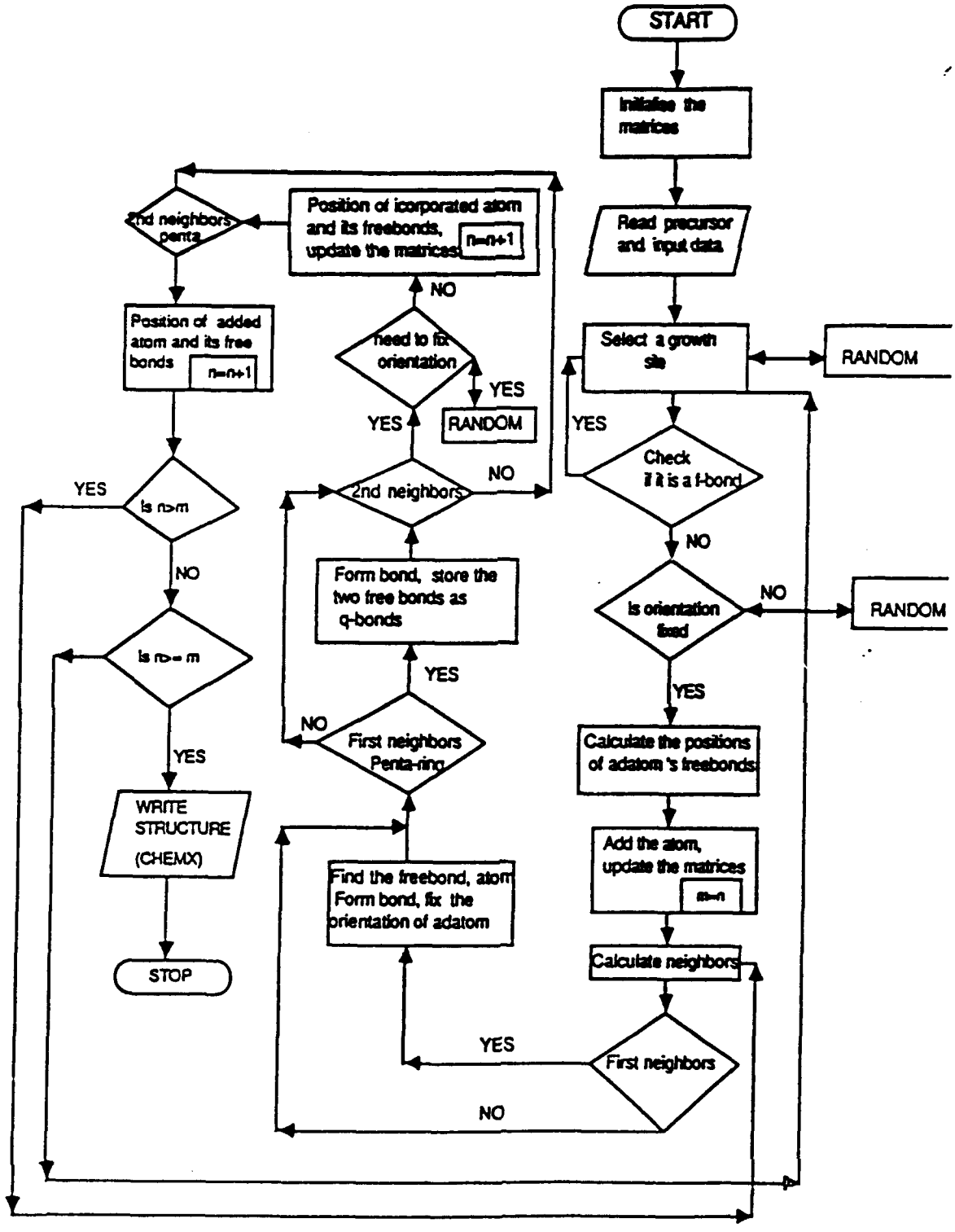

Figure 1. Flow chart of rule–based computer simulation of diamond growth.

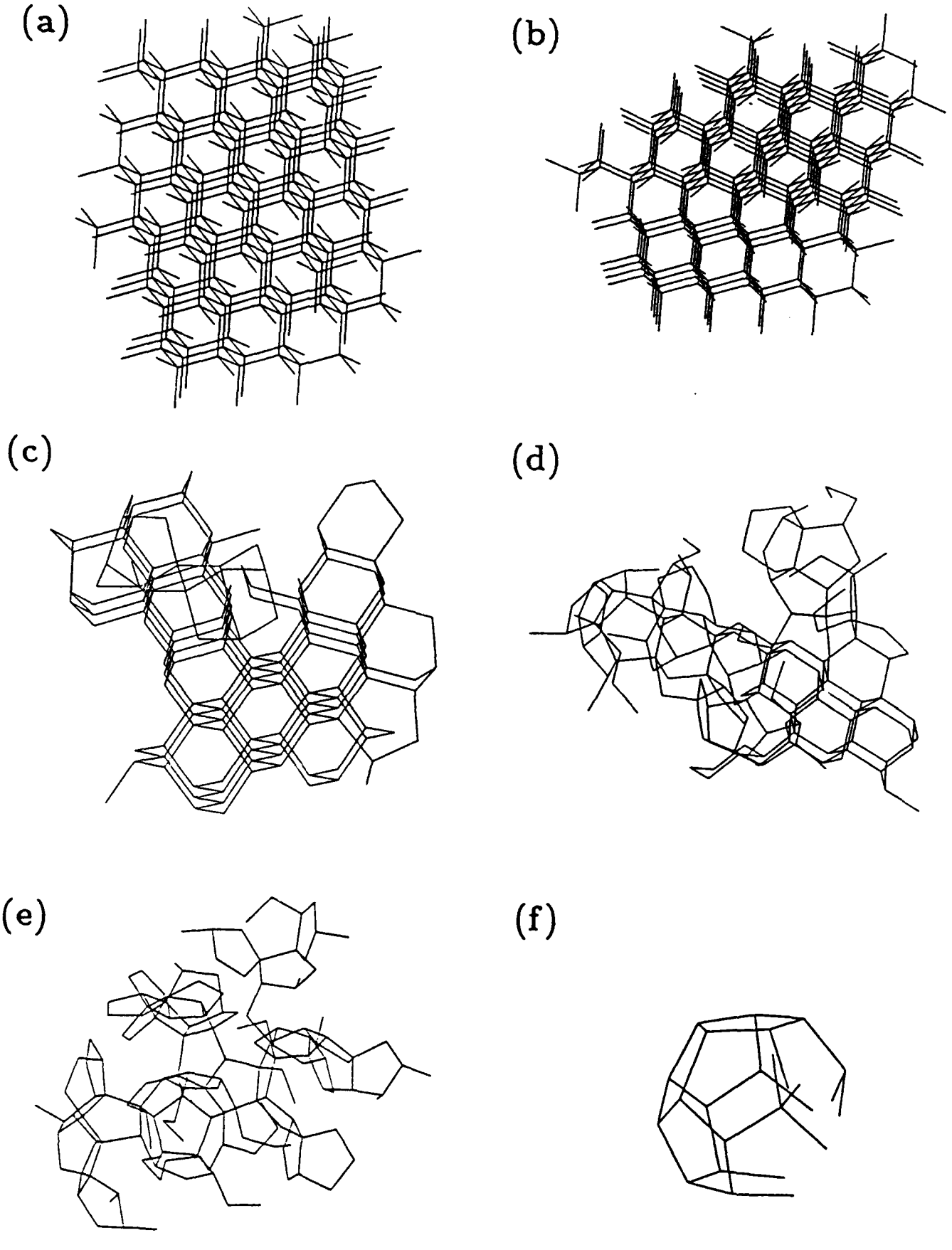

Figure 2. Diamond crystals grown on the computer using different probabilities, P_s, of stacking errors 2a) $P_s = 0$; 2b) $P_s = 0.10$; 2c) $P_s = 0.25$; 2d) $P_s = 0.50$; 2e) $P_s = 1.0$; 2f) small fragment of structure shown in 2e.

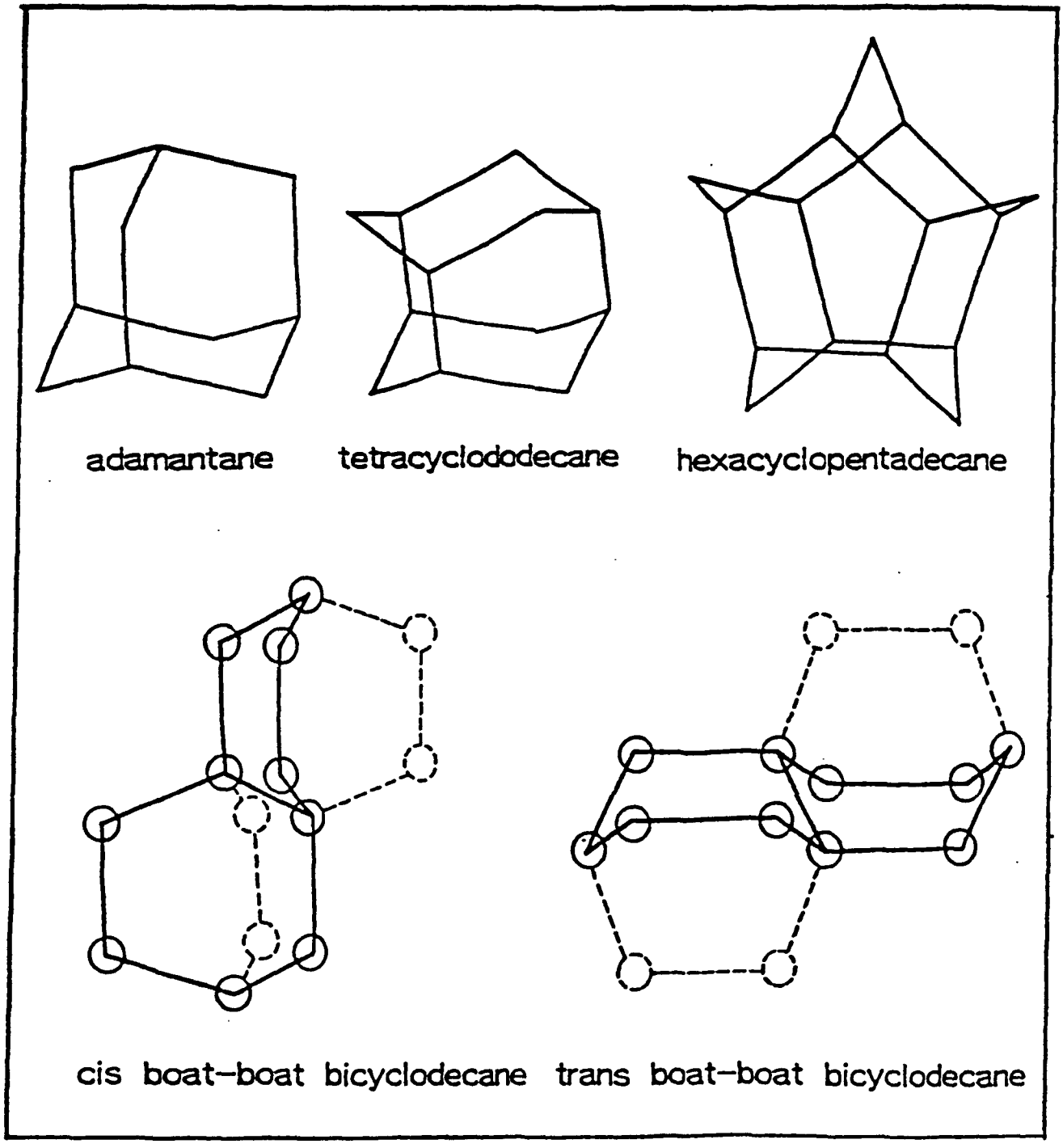

Figure 3. Various precursors proposed as diamond nuclei. Top row shows the cage compounds proposed by Matsui and Matsumoto (3). The bottom row shows the boat–boat conformers of bicyclodecane proposed by Angus (1,2).

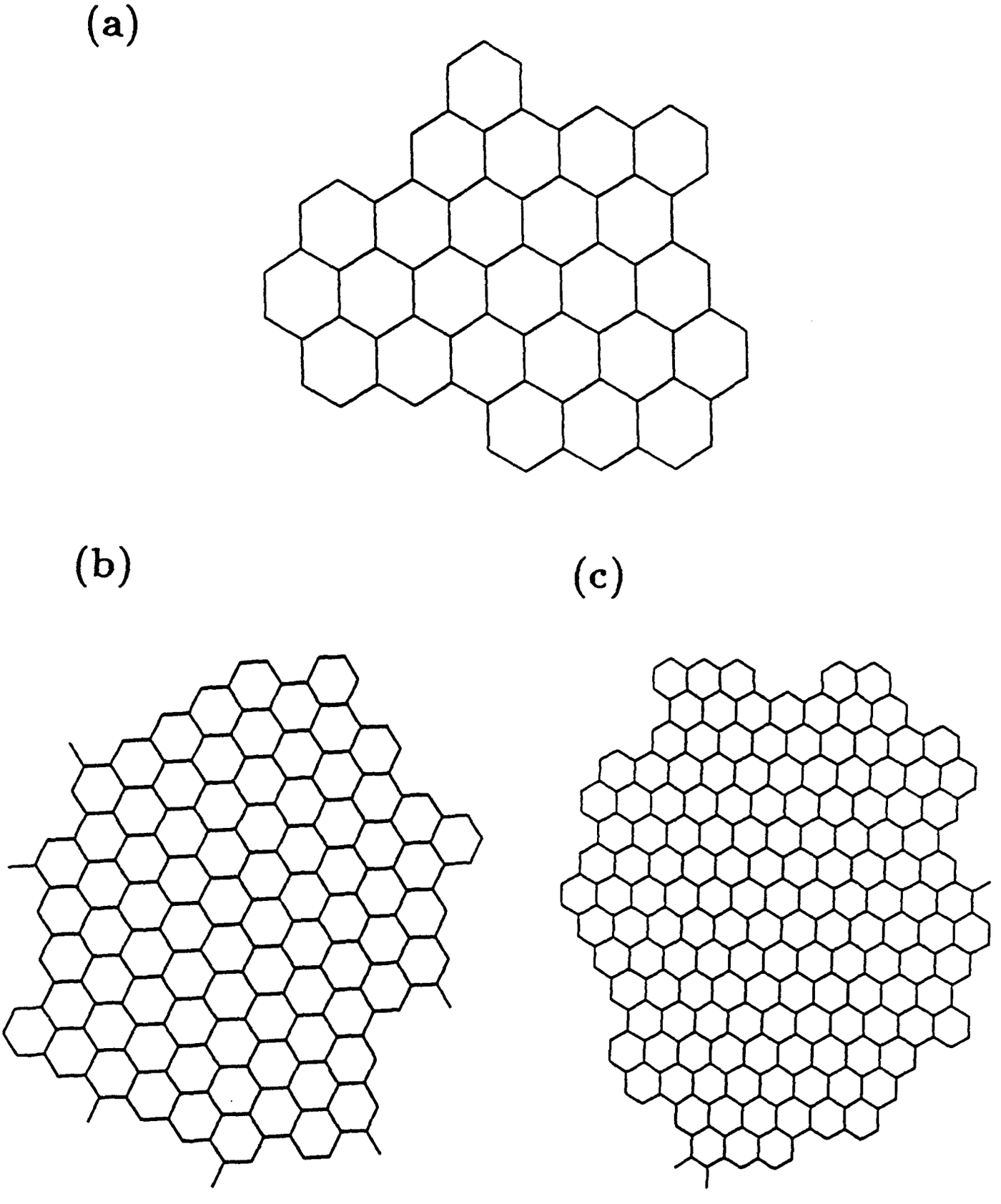

Figure 4. Crystals grown from precursor of Figure 3. 4a) 200 added atoms; 4b) 600 added atoms; 4c) 1000 added atoms. The crystallites are viewed normal to the double twin plane. Each crystallite is 3 layers deep.

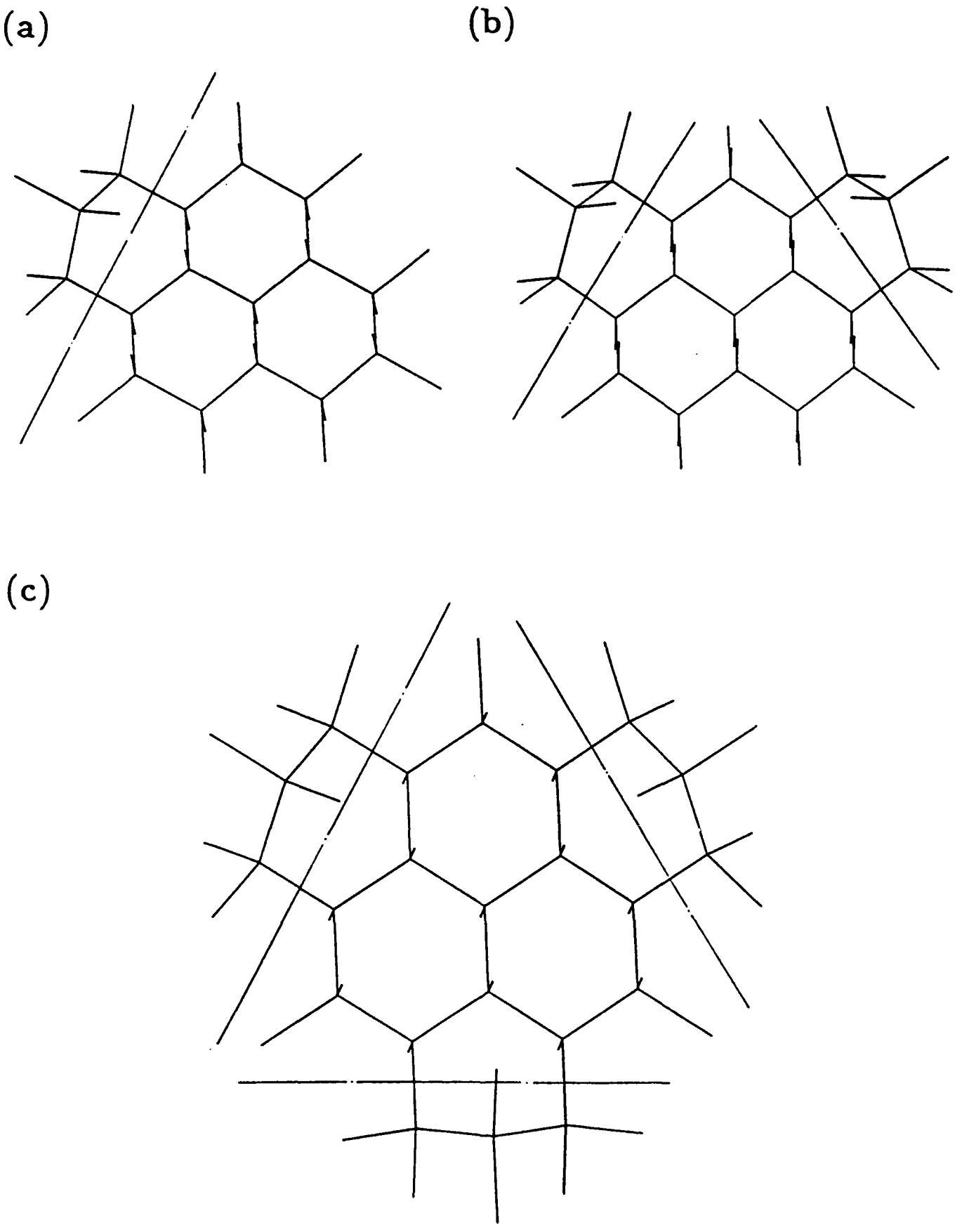

Figure 5. Twinned precursor nuclei. 5a) singly twinned nucleus; 5b) doubly–twinned nucleus; 5c) triply–twinned nucleus. The twin planes are indicated by a dashed line.

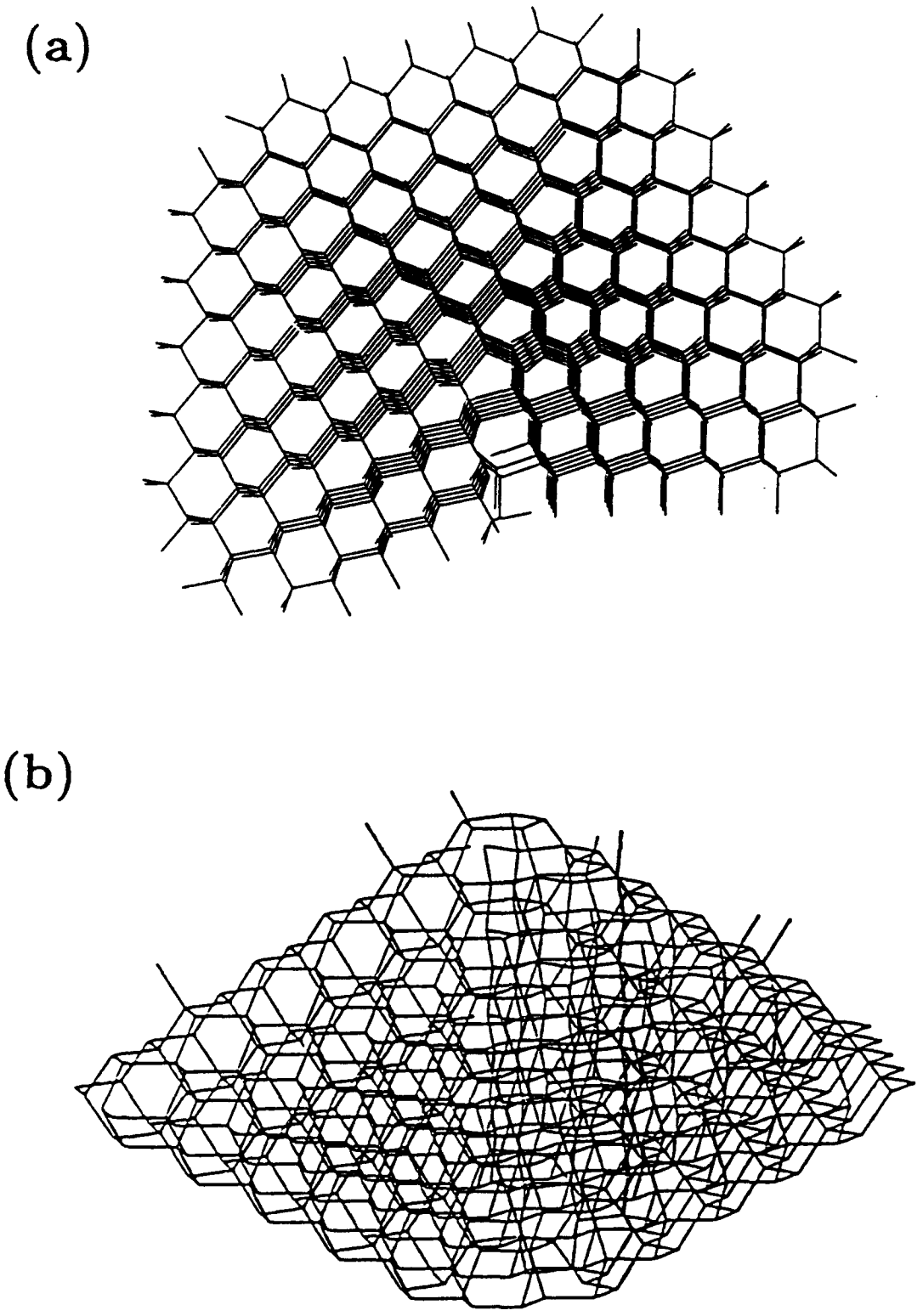

Figure 6. Five–fold twinned decahedral crystal arising from doubly–twinned nucleus shown in Figure 5b. 6a) top view; 6b) side view.

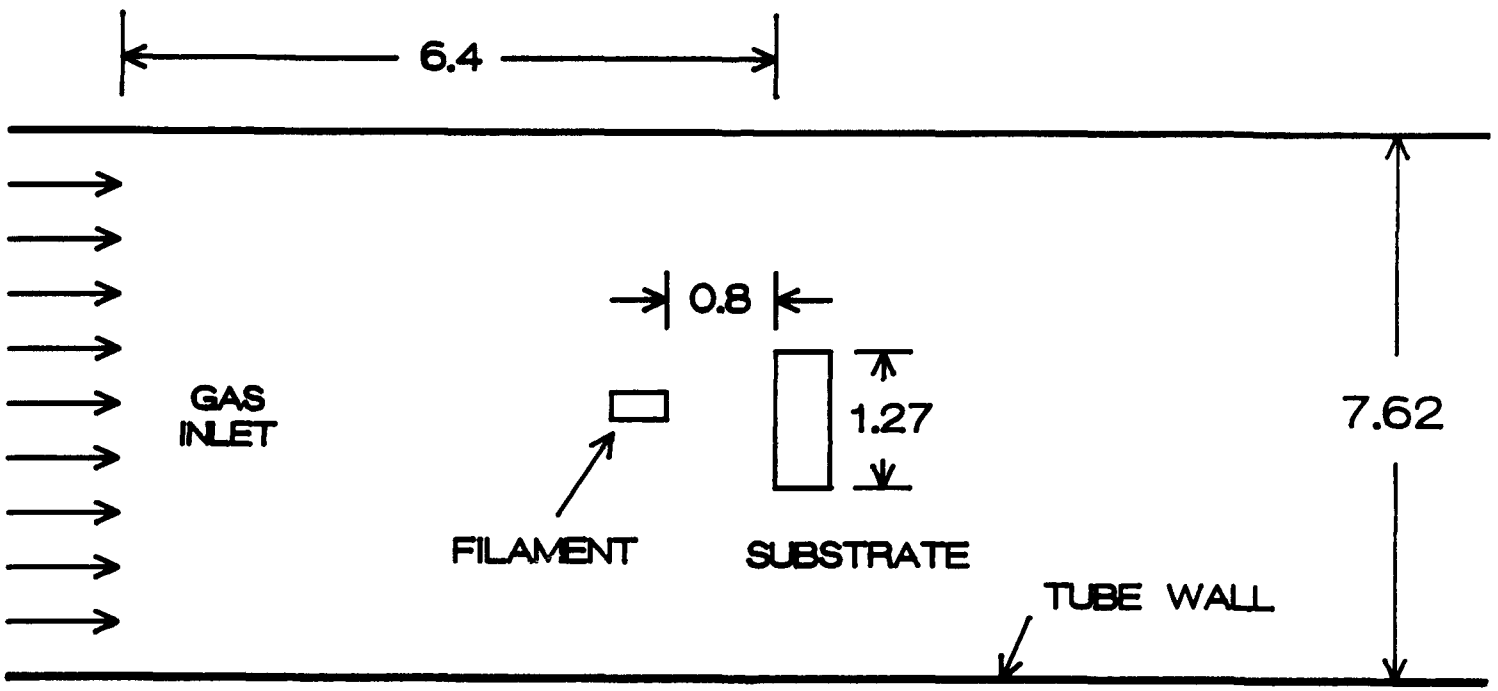

Figure 7. Schematic diagram of tubular hot-filament diamond deposition reactor used for simulation studies. All dimensions are in centimeters.

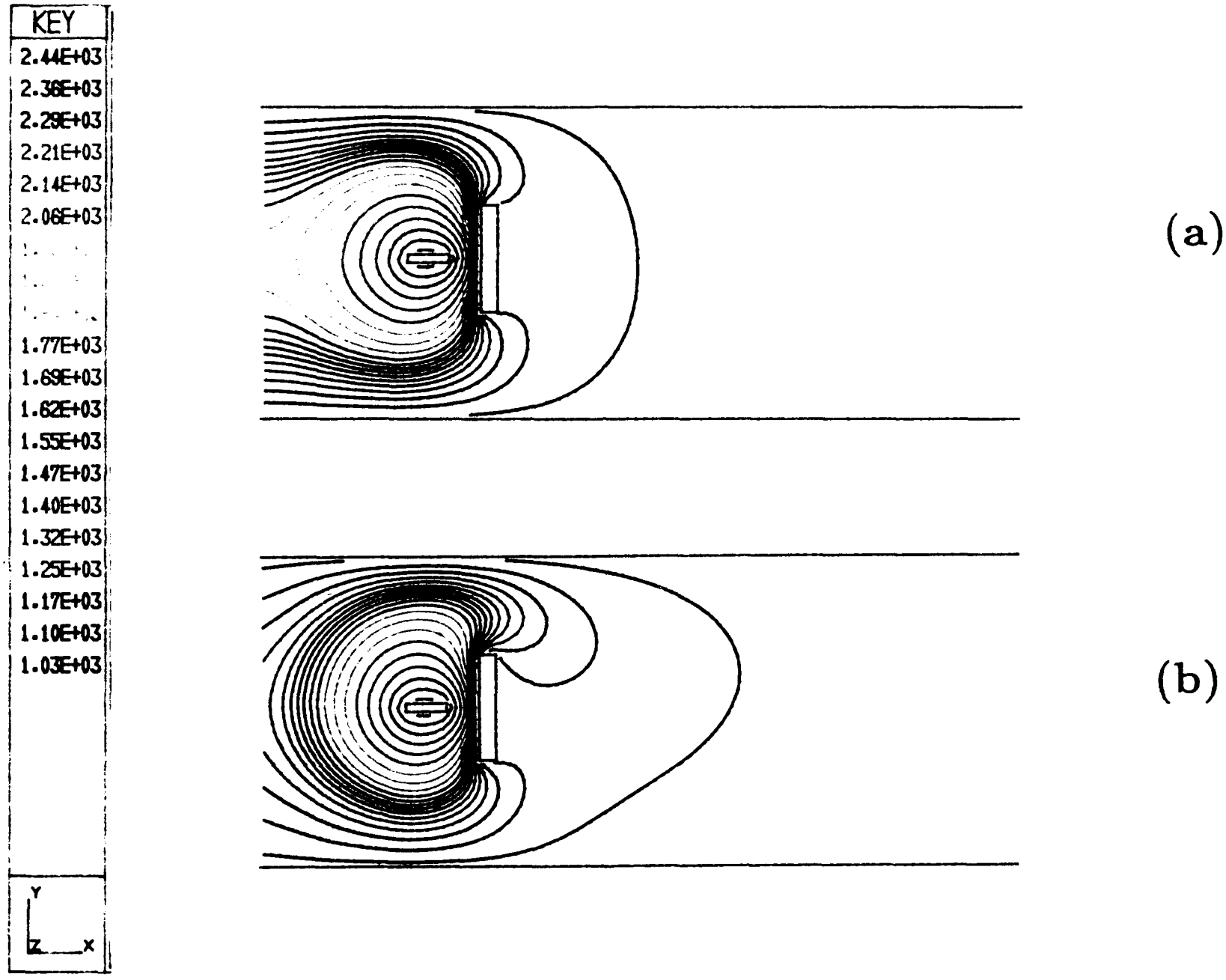

Figure 8. Computed temperature contours in hot-filament diamond deposition reactor. 8a) P = 20 Torr; 8b) P = 760 Torr. Temperatures in °K. Note colored scale on left for interpreting the colored contour lines.

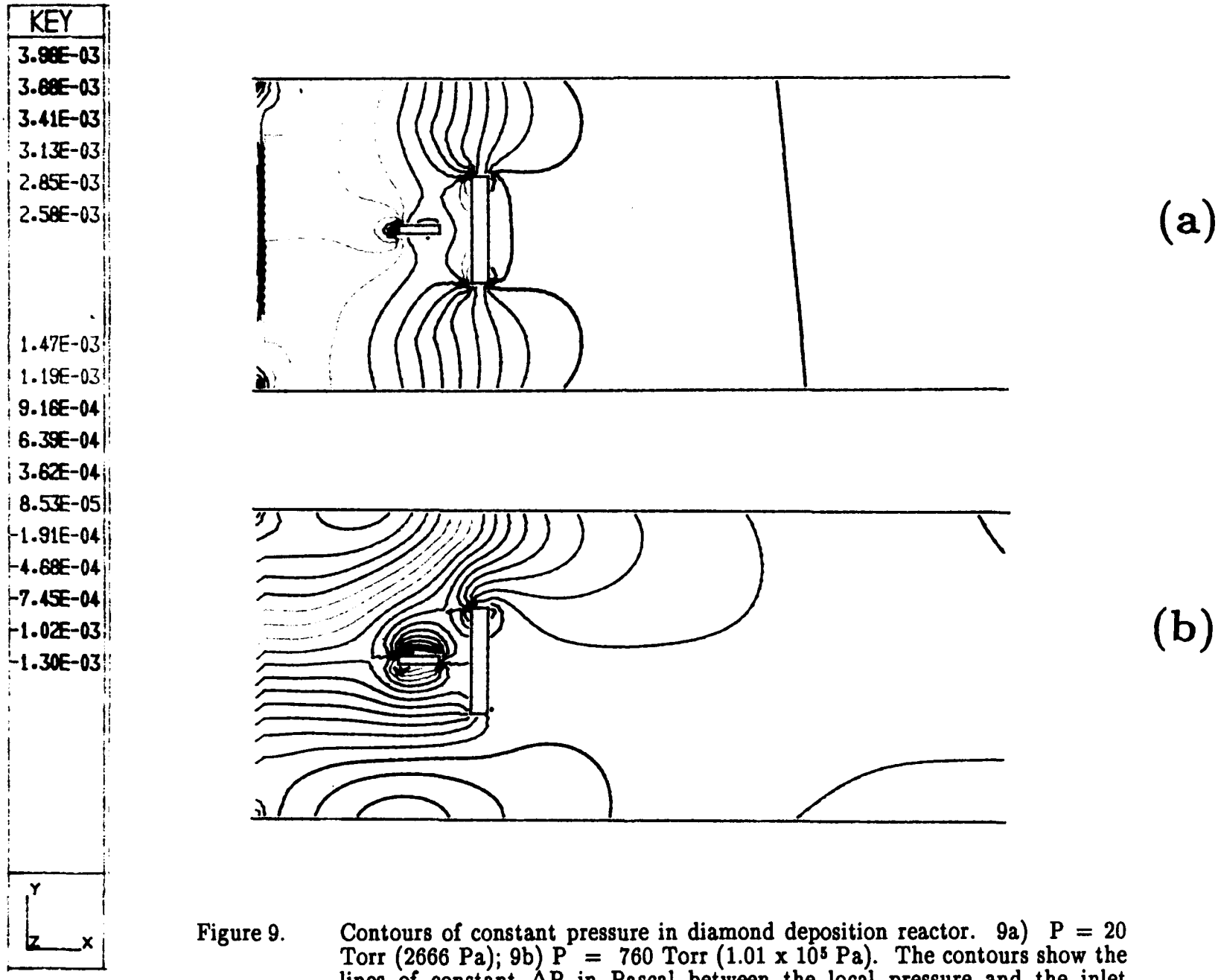

Figure 9. Contours of constant pressure in diamond deposition reactor. 9a) P = 20 Torr (2666 Pa); 9b) P = 760 Torr (1.01×10^5 Pa). The contours show the lines of constant ΔP in Pascal between the local pressure and the inlet pressure of 2666 Pa. Note colored scale on left for interpreting the colored contour lines.

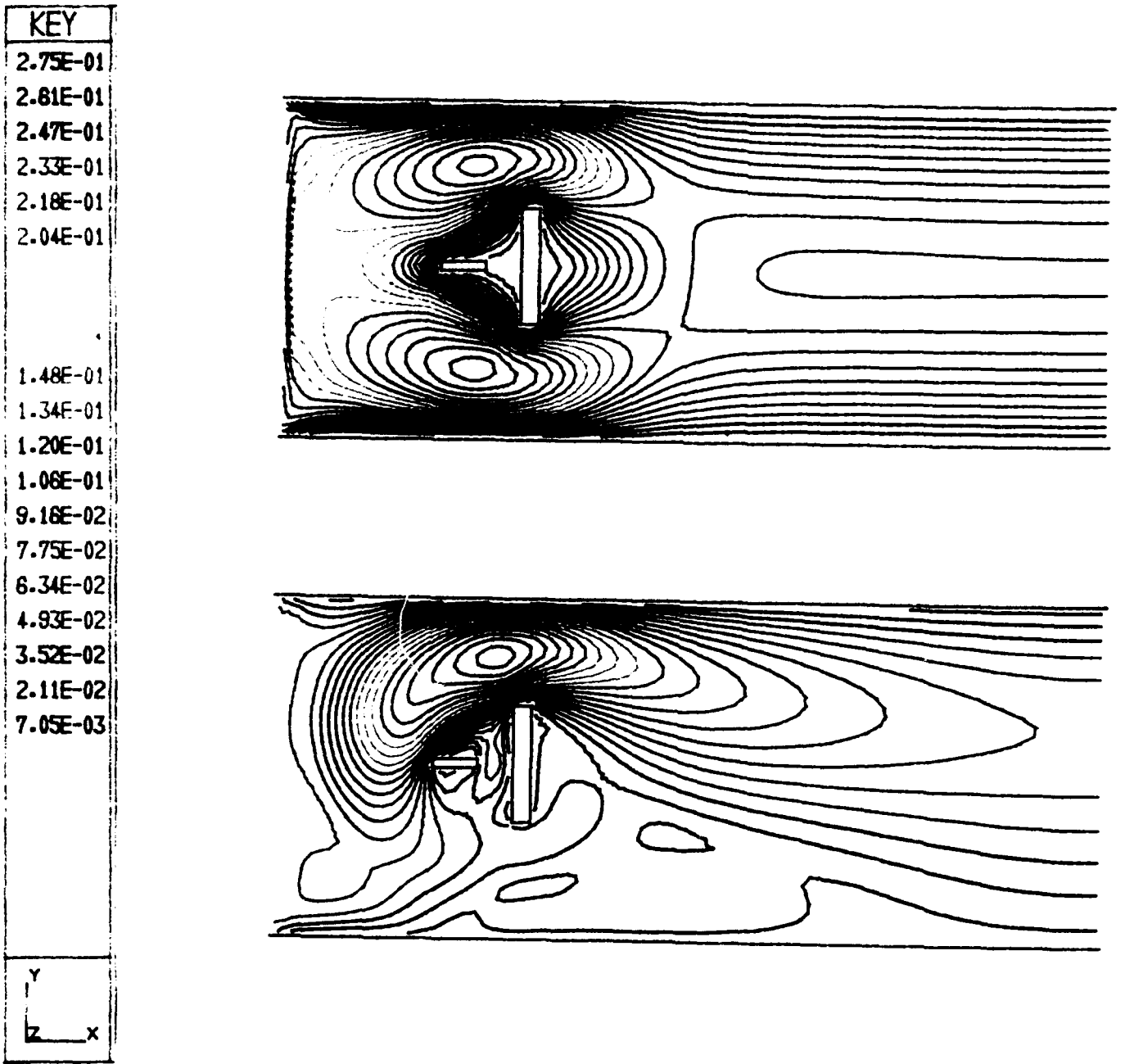

Figure 10. Contours of constant axial velocity in diamond deposition reactor. 10a) P = 20 Torr; 10b) P = 760 Torr. Velocities in m/sec. Note colored scale on left for interpreting the colored contour lines.

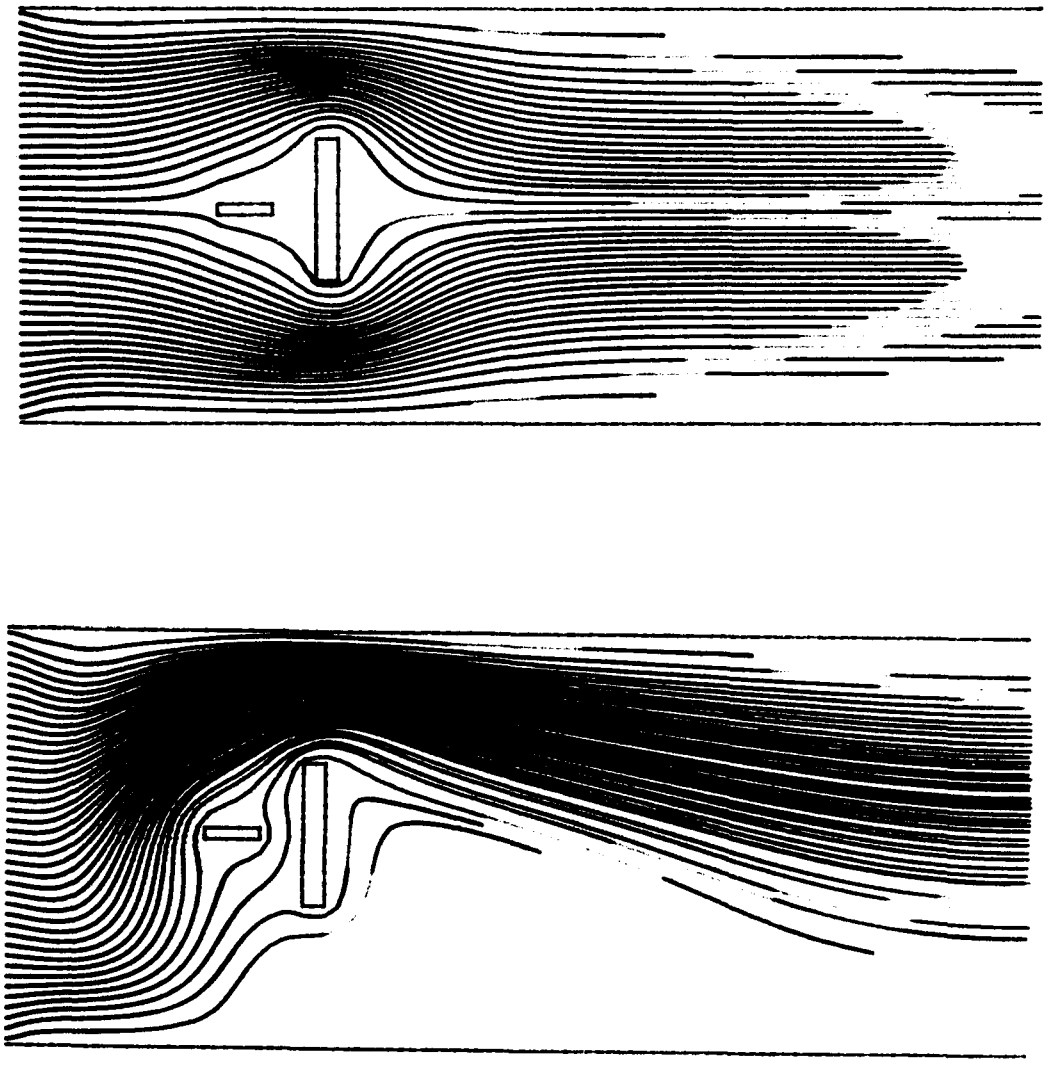

Figure 11. Streamlines in diamond deposition reactor. 11a) P = 20 Torr; 11b) P = 760 Torr. Note significant convection at 760 Torr compared to 20 Torr.

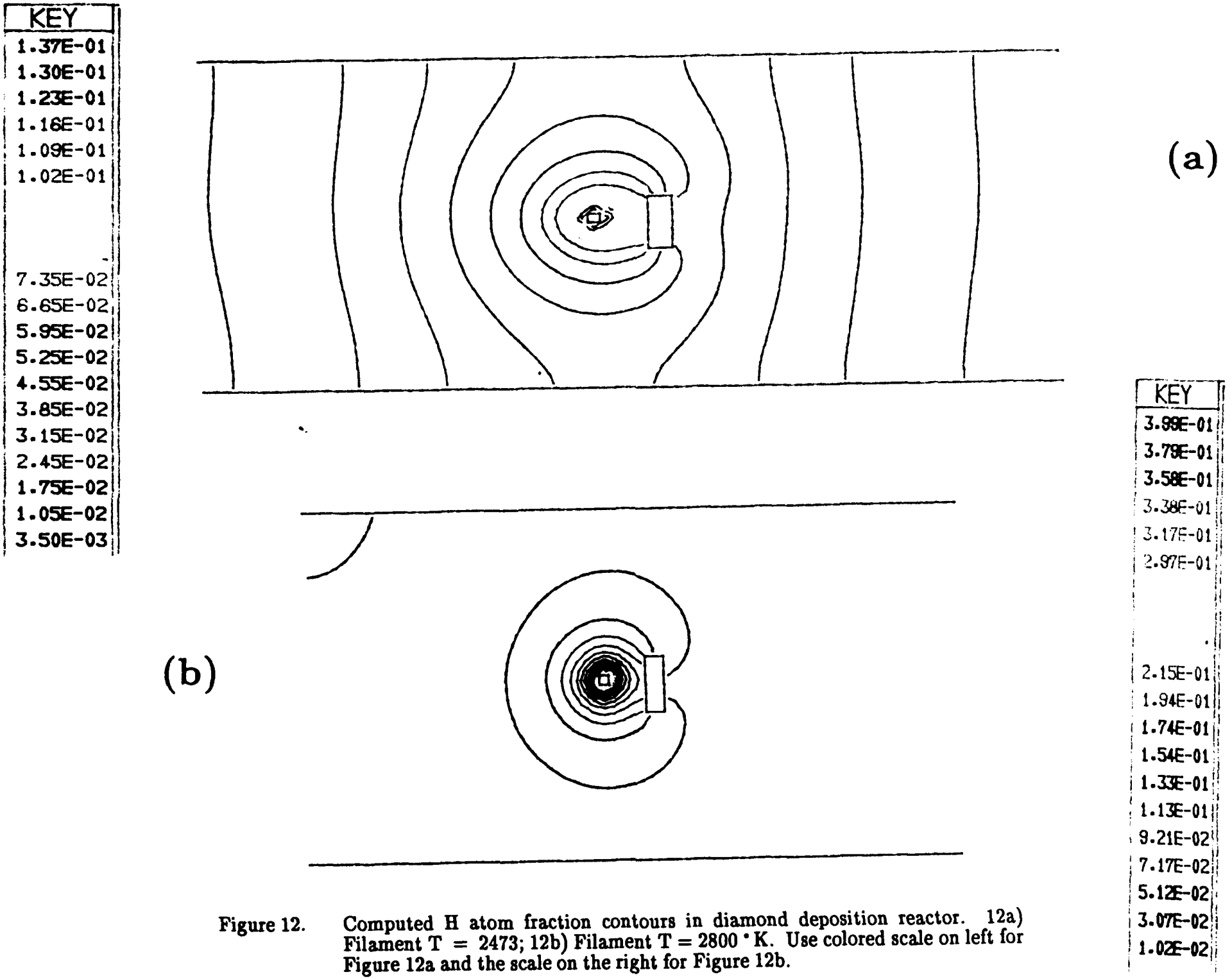

Figure 12. Computed H atom fraction contours in diamond deposition reactor. 12a) Filament T = 2473; 12b) Filament T = 2800 °K. Use colored scale on left for Figure 12a and the scale on the right for Figure 12b.

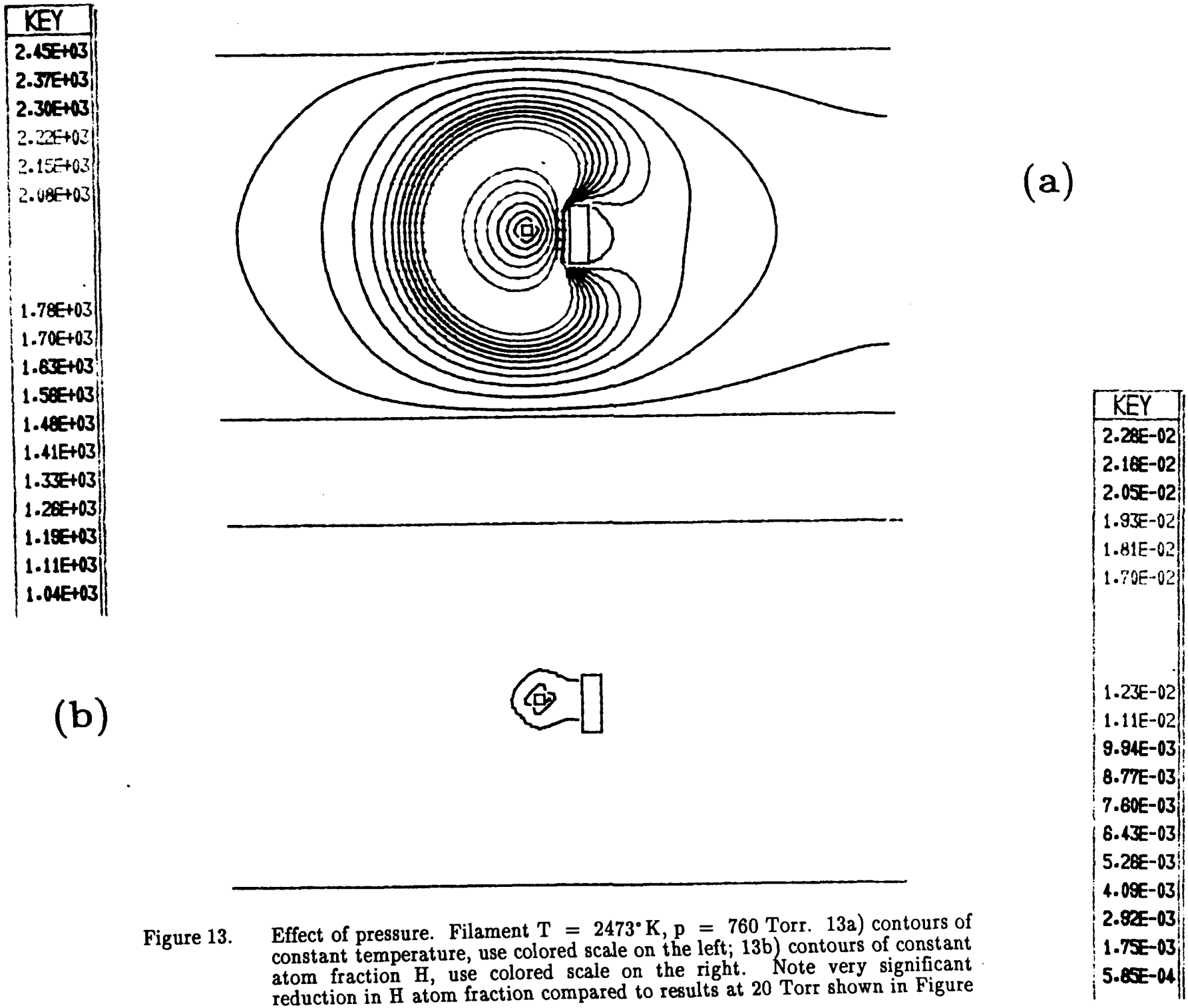

Figure 13. Effect of pressure. Filament T = 2473°K, p = 760 Torr. 13a) contours of constant temperature, use colored scale on the left; 13b) contours of constant atom fraction H, use colored scale on the right. Note very significant reduction in H atom fraction compared to results at 20 Torr shown in Figure

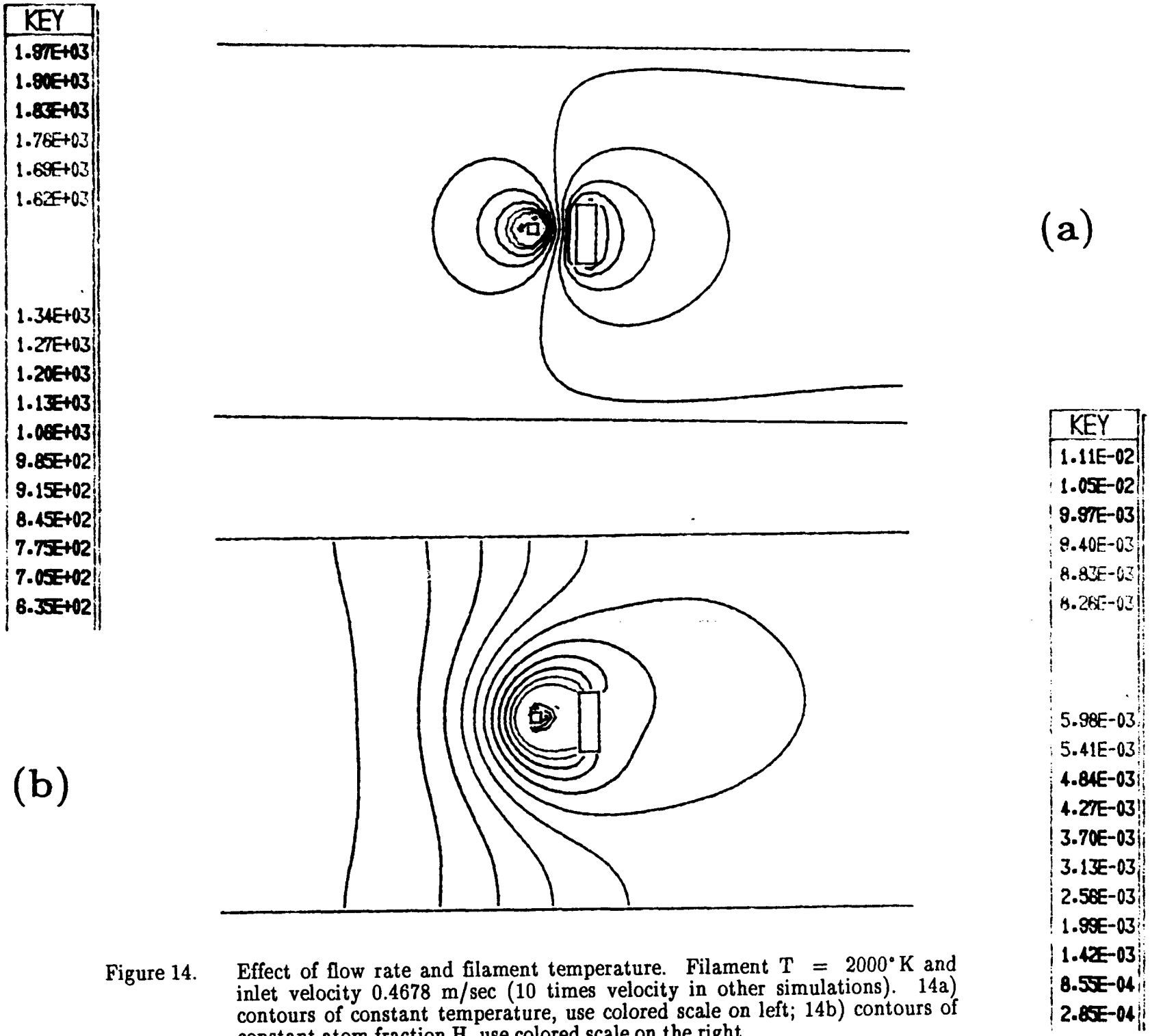

Figure 14. Effect of flow rate and filament temperature. Filament T = 2000°K and inlet velocity 0.4678 m/sec (10 times velocity in other simulations). 14a) contours of constant temperature, use colored scale on left; 14b) contours of constant atom fraction H, use colored scale on the right.

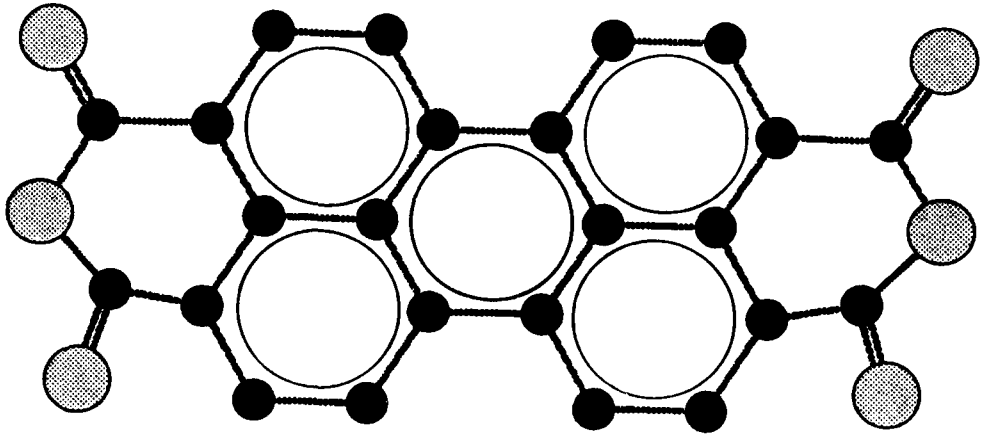

Figure 15. Molecular structure of 3, 4, 9, 10–perylene tetracarboxylic acid dianhydride (PTCDA).